

# Acceleration of a ground-state reaction by selective femtosecond infrared laser excitation

Till Stensitzki,<sup>1</sup> Yang Yang,<sup>1</sup> Valeri Kozich,<sup>1</sup> Ashour A. Ahmed,<sup>2,3</sup> Florian Kössl,<sup>1</sup> Oliver Kühn<sup>3</sup> & Karsten Heyne<sup>1\*</sup>

<sup>1</sup> Freie Universität Berlin, Department of Physics, Arnimallee 14, 14195 Berlin, Germany

<sup>2</sup> University of Cairo, Faculty of Science, Department of Chemistry, 12613 Giza, Egypt

<sup>3</sup> University of Rostock, Institute of Physics, Albert Einstein-Str. 23-24, 18059 Rostock, Germany

**Infrared (IR) excitation of vibrations that participate in the reaction coordinate are believed to accelerate an otherwise thermally driven chemical reaction. Attempts of practical realization of this concept have been hampered so far by competing processes leading to sample heating. Here we demonstrate, using femtosecond IR-pump IR-probe experiments, the acceleration of urethane and polyurethane formation due to vibrational excitation of the reactants for 1:1 mixtures of phenylisocyanate and cyclohexanol, and toluene-2,4-diisocyanate and 2,2,2-trichloroethane-1,1-diol, respectively. We determined reaction rate changes upon selective vibrational excitation with negligible heating of the sample and observed an increase of the reaction rate up to 24%. The observation is rationalized using reactant and transition state structures obtained from quantum chemical calculations. We utilized reaction acceleration to write a polyurethane square on sample windows by a femtosecond IR pulse.**

New cost-effective methods for synthesis of molecular films or three-dimensional architectures with specific properties are in demand. For example, IR laser induced synthesis of graphene has been demonstrated, utilizing photothermal effects at high temperatures to manufacture films with high electrical conductivity<sup>1</sup>. A standard tool in imaging and radiation curing technologies is photopolymerization<sup>2-5</sup>. Here, the polymerization reaction is triggered or accelerated by the absorption of visible light. In most cases, this involves photochemistry via excited electronic states<sup>2-5</sup>, i.e. with radical formation, dissociation of molecules or via high vibrational overtones<sup>6-11</sup>. A reduction of photon numbers and energy would decrease the costs of laser-based methods. This should be possible by controlling thermally driven reactions by a single photon with moderate energy as provided by the IR spectral region.

Many chemical reactions are driven by thermal activation<sup>12-14</sup>. In a simplified picture, a ground-state reaction proceeding from reactants such as phenylisocyanate (PHI) and cyclohexanol (CH-ol) to a product (here cyclohexyl-carbanilate, CC) can be expressed as a transformation on an energy surface from a reactants' energy minimum to a product energy minimum through a transition state (cf. Fig. 1). Thereby, the reaction coordinate (RC) traces the reaction pathway with the lowest energy. Elevated temperatures increase the collision rate and hence the population of vibrational modes of higher energy participating in the RC. Thus, nuclear conformations can be reached that are associated

with the transformation from reactants to the transition state and thermal energy propels the system over the transition state to the product.

While temperature dependence of a chemical reaction in solution provides important information on the reaction rate and activation barrier<sup>12,13</sup>, details on the RC, on the nuclear conformation, and the dynamics of the reactive complex and its surroundings at the transition state (TS) are hard to obtain for ground state reactions<sup>15</sup>.

It is known that coherent excitation pulses can be applied to select and optimize specific molecular reaction pathways. Coherent control strategies were developed for electronic ground and excited states (for reviews, see refs. 16-20). Recently, it was shown that mode specific excitation of vibrations coupled to electron transfer pathways in an excited electronic state can efficiently change the outcome of a reaction<sup>21,22</sup>.

In contrast, acceleration of thermally driven ground state reactions without heating all molecules is very difficult. Heating the sample results in excitation of vibrational modes according to the Boltzmann distribution. In comparison, direct IR excitation instantaneously populates a specific vibrational mode<sup>23-25</sup>. Relaxation of the excited mode occurs via intramolecular vibrational energy redistribution (IVR) on a picosecond (ps) time scale and intermolecular vibrational energy relaxation (VER, also called intermolecular energy transfer, IET) into a microvolume around the excited molecule on a longer time scale<sup>26-31</sup>. Hence, to distinguish between excitation of RC and heating, time resolved experiments with ultrafast time resolution are necessary. Thus, femtosecond (fs) IR excitation is a promising tool to initiate and track otherwise thermally driven chemical reactions via direct excitation of the RC. However, there are only very few successful experimental realizations of fs IR pulse initiated reactions, which are limited to small molecules undergoing simple unimolecular reactions. For instance, Motzkus et al. demonstrated vibrational ladder climbing enhancing the statistical dissociation yield of Cr(CO)<sub>6</sub> decarbonylation<sup>23</sup>. In a pioneering work, the same group also demonstrated nonstatistical dissociation of CH<sub>2</sub>N<sub>2</sub>, but in gas phase<sup>32</sup>. Furthermore, Hamm et al. used IR laser pulses to drive the cis-trans-isomerization of HONO in a Kr matrix at 32 K<sup>33</sup>. Up to now, IR pulse driven reactions were limited to unimolecular systems in the condensed phase.

In this study, for the first time, we present evidence for acceleration of urethane and polyurethane formation by direct ultrafast IR excitation of the alcohol OH-stretching vibration and the isocyanate NCO-stretching vibration, respectively. At these spectral positions, solvent absorption is negligible.

The outcome of a thermally driven reaction can be influenced by changing temperature, concentrations and solvent. These concepts are often insufficient, e.g. for chemical synthesis of thermally instable products.

We break new ground in condensed phase synthesis via IR excitation of vibrations participating in the RC. Since continuous-wave (cw) IR laser sources are easily available, IR excitation of such vibrations should make it possible to accelerate a synthesis reaction without heating the solvent. Moreover, it should be possible to select a specific reaction within a set of competing reactions provided that they correspond to different projections of the RC onto the vibrational modes. The vibrations participating in the RC can be determined experimentally or via quantum chemical calculations.

## Results and discussion

Two thermally driven bimolecular reactions (BMR) were investigated: the reaction between PHI and CH-ol in tetrahydrofuran (THF), and the step-growth reaction between toluene-2,4-diisocyanate (TDI) and 2,2,2-trichloroethane-1,1-diol (chloralhydrate, TCD) in a mixture of nitrobenzene, cyclohexane, and chloroform, leading to urethane (CC), and polyurethane formation, respectively (see Fig. 1, and Supplementary Figs. 1 and 4). Both, the reactions between PHI and CH-ol, as well as between TDI and TCD show second-order kinetics and are thermally activated at room temperature. The experimental Arrhenius activation energy is  $2340 \pm 70 \text{ cm}^{-1}$ , i.e.  $(6.7 \pm 0.2) \text{ kcal/mol}$ , and  $980 \pm 10 \text{ cm}^{-1}$ , i.e.  $(2.80 \pm 0.03) \text{ kcal/mol}$ , respectively<sup>34</sup>.

In order to shine light into the mechanistic details of the initial step of the alcoholysis and polymerization reaction and to identify vibrations connected to this reaction, we have performed a quantum chemical study for PHI reacting with CH-ol in THF. For reactions of isocyanates with alcohols, the reported theoretical and experimental values for free energies of activation differ considerably. Applying density functional theory either for the reaction in the gas phase or embedded into a polarizable continuum model results in energies differing by a factor of three or larger (for a literature overview, see ref. 34). Our calculations provide nuclear conformations and energetics for the stationary points of the reaction of PHI and CH-ol in an *explicit* THF solvent as presented in Fig. 2. Apparently, both the reactant state (called R2) and the transition state have a cyclic structure with a weak hydrogen bond between the OH group of the alcohol and the nitrogen atom of the isocyanate group. The calculated Gibbs energy of activation for this reactant state is 6.8 kcal/mol, i.e. in rather good agreement with the reported experimental value<sup>34</sup>. In view of the many unsuccessful attempts to obtain activation energies that are close to experiment, this clearly points to the importance of including explicit solvent molecules (see Supplementary Figs. 5-7 and Supplementary Tables 1-5).

Unfortunately, the cyclic nuclear conformation of the reactant R2 providing a low Gibbs free energy (about  $2300 \text{ cm}^{-1}$  (6.8 kcal/mol)) belongs to a minor fraction in solution according to the calculations. The majority species, R1, is more likely to be an open configuration (cf. Fig. 2) with a Gibbs free energy of about  $4700 \text{ cm}^{-1}$  (13.4 kcal/mol). This already points to a potentially low overall quantum yield for CC urethane formation upon IR excitation. Further, as detailed in Supplementary Table 4, the

interaction of the solvent in the R2 and TS conformations is stronger for CH-ol than for PHI. Nevertheless, the conformational change between R2 and TS is small for CH-ol compared to PHI, where conformational changes of the NCO group are observed. These conformational alterations from R2 to TS suggest a stronger influence of the NCO-stretching vibration,  $\nu(\text{NCO})$ , on the RC compared to the OH-stretching vibration,  $\nu(\text{OH})$ .

Since the vibrational energy of  $\nu(\text{OH})$  is above the activation energy of R2 and we expect the  $\nu(\text{OH})$  of CH-ol to be part of the RC, its excitation should result in an increase of the reaction rate. In the following, we compare the reaction rate at room temperature with and without fs IR light excitation. In Fig. 3a the OH-stretching  $\nu(\text{OH})$  band absorption of CH-ol is presented as a function of time after mixing CH-ol with PHI for 0 and 300 min (black lines) in THF (for more time steps see Supplementary Figs. 11, and 14). The  $\nu(\text{OH})$  absorption band of CH-ol at  $3470 \text{ cm}^{-1}$  decreases, while the NH-stretching absorption  $\nu(\text{NH})$  of CC at  $3300 \text{ cm}^{-1}$  increases (for a band assignment, see ref. 34). The rise of the strongest product band at  $1730 \text{ cm}^{-1}$  due to the  $\nu(\text{CO})$  vibration of CC, and the band due to the  $\delta(\text{NH})$  vibration of CC at  $1505 \text{ cm}^{-1}$  are presented in Fig. 3b and Supplementary Fig. 11, as well as the decrease of the band due to the  $\nu(\text{NCO})$  &  $\delta(\text{CH})$  vibrations of PHI at  $1512 \text{ cm}^{-1}$ . Excitation of an exact duplicate of this sample by IR pulses of  $\sim 3 \mu\text{J}$  at  $3500 \text{ cm}^{-1}$  leads to a speed up of absorption decrease of CH-ol and PHI bands and absorption increase of CC bands (red lines).

The acceleration of the reaction was determined by the ratio of the reaction rates with and without fs IR pulse illumination. We measured an acceleration of  $(24 \pm 7)\%$  upon illumination with IR light around  $3470 \text{ cm}^{-1}$  (Supplementary Fig. 11).

To exclude multi-photon absorption, we changed the focal diameter from 0.2 mm to 1-2 mm and detected no change of the acceleration. According to the Arrhenius law, a temperature increase of about  $6^\circ\text{C}$  (of the full sample) is needed to increase the reaction rate by 24% for PHI and CH-ol (see Supplementary section 3.5.1). The estimated temperature increase upon fs IR excitation in the focal volume of the sample using heat capacity and absorbed energy is less than  $1^\circ\text{C}$  (Supplementary Section 3.5.3). Moreover, we detected no heating of the focal volume over time (see Supplementary Fig. 12). Nevertheless, adding vibrational energy of  $3500 \text{ cm}^{-1}$  into the  $\nu(\text{OH})$  of CH-ol, can lead to transient local heating of a microvolume around the absorbing molecule<sup>28</sup> accelerating the thermally driven reaction.

Since local heating by light absorption is a time-dependent process, we investigated the *ultrafast dynamics* of CH-ol and PHI in THF. Excitation of the CH-ol  $\nu(\text{OH})$  vibration, which has a lifetime of about 4 ps (see Supplementary Fig. 16), can either (i) initiate directly the BMR with H-bonded PHI if the cyclic nuclear conformation of the reactant R2 is adopted, (ii) excite vibrational modes of the separate reactant CH-ol with lower energy via IVR, (iii) excite vibrations of already formed H-bonded CC via VER, or (iv) excite vibrations of other molecules in the sample, mainly THF via VER leading to heating of the solvent and the complete sample.

Direct tracking of the first reaction step should be possible by fs IR-pump IR-probe experiments. This method is highly sensitive to transient changes in the IR absorption. The expected signal upon excitation with a single fs IR pulse at  $3500 \text{ cm}^{-1}$  can be estimated by the absorption change from Fig. 3b and

Supplementary Fig. 14 to about 0.1 to 0.3 mOD at 1512  $\text{cm}^{-1}$  (see Supplementary Section 3.5.5). In Fig. 4 we present fs IR-pump IR-probe experiments upon excitation of the OH-stretching vibration  $\nu(\text{OH})$  of CH-ol at 3500  $\text{cm}^{-1}$  (pulse spectrum in Supplementary Fig. 14). Since the signals are very small (cf. Supplementary Figs. 21 and 22), we averaged difference absorbance spectra within specific delay time intervals. The difference absorbance spectra are shown for delay times around 3 ps (red dots), around 13 ps (green squares), around 38 ps (wine circles), and for long delay times around 76 ps (blue open squares).

Excitation of the  $\nu(\text{OH})$  results in a broad positive signal around 1500  $\text{cm}^{-1}$  due to strong absorption changes of the  $\delta(\text{CH})$  of CH-ol at 1450  $\text{cm}^{-1}$  (see Supplementary Fig. 16), and a distinct bleaching signal of 0.1 mOD around 3 ps due to the  $\nu(\text{NCO})$  &  $\delta(\text{CH})$  vibrations of PHI at 1512  $\text{cm}^{-1}$  in Fig. 4a. The bleaching signal at 1512  $\text{cm}^{-1}$  around 3 ps is not accompanied by a positive signal, which would indicate vibrational excited state absorption, hot ground state absorption, or anharmonic coupling<sup>27,30,35</sup>. Thus, upon  $\nu(\text{OH})$  excitation of CH-ol about 0.1 mOD of the  $\nu(\text{NCO})$  &  $\delta(\text{CH})$  vibrational band of PHI disappears due to BMR, matching roughly the estimated signal for PHI consumption due to accelerated reaction. No bleach recovery is visible demonstrating a high quantum yield (above 50%) for this process. We observe a rise of the bleaching signal and the rise of an absorption band at 1505  $\text{cm}^{-1}$  with a time constant of about (10  $\pm$  3) ps. At 1505  $\text{cm}^{-1}$  the NH-bending vibration,  $\delta(\text{NH})$ , of CC absorbs, indicating the production of CC via BMR in the ground state.

The absorbance change of the NCO-stretching vibration,  $\nu(\text{NCO})$ , around 2270  $\text{cm}^{-1}$  upon  $\nu(\text{OH})$  excitation of CH-ol is depicted in Fig. 4b. An instantaneous negative signal is observed at 2260  $\text{cm}^{-1}$ , and a positive signal at 2240  $\text{cm}^{-1}$ . These features deviate significantly from IVR signals observed upon direct vibrational excitation of NCO (see Supplementary Fig. 17) and we therefore associate these to the consumption of NCO due to BMR and to a minor part VER from CH-ol to PHI. With a time constant of (10  $\pm$  3) ps the bleaching signal rises up to 0.90 mOD, demonstrating consumption of the NCO group. Since the strong bleaching signal increase has no corresponding rise of a positive signal, bleaching via VER can be ruled out, corroborating BMR.

The CH-ol and PHI sample exhibits an increasing amount of thermally formed CC with time. The OH group of CH-ol forms a H-bond with the CO group of the CC (see Supplementary Fig. 15). Thus,  $\nu(\text{OH})$  excitation of CH-ol results in heating of already formed CC via VER and a blue-shift of its  $\nu(\text{CO})$  absorption band (see Supplementary Fig. 13 and 19). To observe only the CC formation due to fs IR pulse excitation, we subtracted two identical measurements with a CH-ol and PHI mixture and a CH-ol and CC mixture (see Supplementary Figs. 19 and 20). The resulting dynamics are free from heating effects of the product and are displayed in Fig. 4c.

At 1730  $\text{cm}^{-1}$ , the rise of the  $\nu(\text{CO})$  absorption is clearly visible. The instantaneous signal (red dots) shows a small amount of  $\nu(\text{CO})$  absorption, and a negative signal at 1710  $\text{cm}^{-1}$  accompanied by a positive signal at 1690  $\text{cm}^{-1}$ . This feature vanishes within a few ps. The  $\nu(\text{CO})$  absorption rises with a time constant of (10  $\pm$  3) ps, demonstrating the CC product formation in the ground state via BMR. From the final CC  $\nu(\text{CO})$  product

signal of 0.75 mOD one can estimate the corresponding bleaching band of the  $\nu(\text{OH})$  to be about 0.125 mOD. Since the total bleaching signal of the  $\nu(\text{OH})$  is expected to be about 35 mOD the overall quantum yield is in the range of 0.3% (see S3.5.6). Note, the quantum yield is concentration dependent (second-order reaction) and decreases with decreasing concentration of both reactants.

The instantaneous signals of the  $\nu(\text{NCO})$  &  $\delta(\text{CH})$  bleaching band at 1512  $\text{cm}^{-1}$ , the  $\nu(\text{NCO})$  bleaching band at 2260  $\text{cm}^{-1}$ , and the  $\nu(\text{CO})$  product band at 1730  $\text{cm}^{-1}$  demonstrate the direct impact of the IR pulse excitation on the CC formation reaction via BMR. The associated time dependencies suggest the formation of CC with (10  $\pm$  3) ps. This time scale is too fast for heating the solvent molecules via VER. In contrast, we observe ultrafast IVR in CH-ol and VER from CH-ol to H-bonded PHI molecules. Since, the instantaneous bleaching signal strength of  $\sim$ 0.1 mOD at 1512  $\text{cm}^{-1}$  equals half of the final bleaching signal, we conclude that a major part of the reaction is directly initiated by the IR pulse excitation and not due to heating processes via other molecules. However, due to our limited time resolution of about 350 fs we cannot unequivocally determine whether the  $\nu(\text{OH})$  of CH-ol is part of the RC or only connected to the RC via IVR or VER. The structures presented in Fig. 2 provide support for the former conclusion.

Reaction acceleration studies were also performed on TCD and TDI in a nitrobenzene/cyclohexane/chloroform solution (Supplementary Figs. 9-11). Since the activation energy of this reaction is 980  $\text{cm}^{-1}$ , several vibrational modes can be excited above the activation energy. We found acceleration of the reaction rates for excitation of the OH-stretching vibration of TCD at 3490  $\text{cm}^{-1}$  of (10  $\pm$  5)% at 0.25 mol/l, and of the NCO-stretching vibration of TDI at 2270  $\text{cm}^{-1}$  of (22  $\pm$  8)% at 0.1 mol/l (Supplementary Fig. 11). No acceleration was observed for excitation at 3070  $\text{cm}^{-1}$ , where the CH-stretching vibrations of TDI and of the solvent nitrobenzene absorb (Supplementary Fig. 11).

A promising and cost effective new application for mid-IR laser induced acceleration of polyurethane formation is photolithography. In Fig. 5 we displayed results of writing polyurethane squares from a 1:1 mixture of TDI and TCD by moving the IR laser spot along the perimeter of a square. Upon variation of the laser focus from  $\approx$  150  $\mu\text{m}$  to  $\approx$  75  $\mu\text{m}$ , the thickness of the polyurethane line is reduced from  $\approx$  160  $\mu\text{m}$  to  $\approx$  80  $\mu\text{m}$ . The polyurethane concentration on the square is more than 20 times higher than elsewhere (Supplementary Fig. 24).

## Conclusions

We demonstrated that selective fs IR excitation of the OH-stretching vibration of the alcohol CH-ol accelerates the CC urethane formation from CH-ol and PHI. This BMR process takes place on the fs to ps time scale. However, the reaction yield is not only concentration dependent, but strongly limited by the molecular conformation of CH-ol and PHI. Only a minor fraction, R2, reacts at photon absorption that adopt a conformation close to the calculated transition state. The major fraction experiences IVR without CC urethane formation. This explains the poor overall quantum yield of about 0.3% upon IR excitation at the OH-stretching vibration. The presented theoretical results corroborate these indications and showed, for the first time, that an accurate

calculation of the activation energy for urethane formation is possible. To this end, it was required to include the solvent molecules explicitly.

For TDI and TCD it was found that excitation of both, the NCO- and the OH-stretching vibrations, accelerate the polymerization reaction. Our data indicated a more efficient acceleration per photon energy upon excitation of the NCO-stretching vibration. This could point to a higher participation to the RC as compared with the OH-stretching vibration.

In contrast to previous attempts getting ahead of IVR<sup>32</sup> we benefit from existing pathways of vibrational energy flow<sup>26</sup> connected to the thermally driven reaction. Direct excitation of the RC or excitation of vibrations efficiently relaxing into vibrations, which are part of the RC, accelerates the otherwise thermally driven reaction. This is a new and simple approach to steer chemical reactions by single photon excitation of the first vibrational excited state. An exhaustive experimental investigation of all involved vibrational relaxation dynamics would allow to characterize those pathways in more detail.

Since a multitude of chemical reaction steps are thermally driven or partly thermally driven, the presented method opens up a variety of new strategies to utilize photons to steer, optimize and localize ground state chemical reactions in solution.

It should be emphasized that, in terms of the number of photons, selective IR excitation provides a cost-effective way for triggering reaction in the electronic ground state. Further extensions include, for instance, the use of polarized laser beams. This might enable to imprint a preferred orientation on the polyurethane by using linear instead of branched diols and diisocyanates.

## Methods

The urethane-group formation due to the alcoholysis reaction is shown in Fig. 1. Equimolar solutions of PHI (Aldrich 98%) and CH-ol (Aldrich 98.5%) in THF (Aldrich 99.9%) with concentrations of about 0.75 mol/l were used for the acceleration studies. We used different concentrations, and spacer thicknesses at different probing wavenumbers for the fs time-resolved experiments presented in Fig.4: (0.05 mm / 0.75 M / 1500 cm<sup>-1</sup> / Fig. 4a), (0.05 mm / 0.375 M / 2270 cm<sup>-1</sup> / Fig. 4b), and (0.1 mm / 1.5 M / 1730 cm<sup>-1</sup> / Fig. 4c).

The acceleration studies were performed with two equimolar solutions of TDI (Sigma ≥ 98%) and TCD (Sigma 99.5-101%) of 0.1 mol/l. For excitation around 2270 cm<sup>-1</sup> and 3070 cm<sup>-1</sup> we used a 2:1:1 mixture of nitrobenzene (Sigma ≥ 99%), cyclohexane (Sigma 99.5%) and chloroform (Sigma 99 %). The same sample with a five times higher concentration was used for writing a polymer square. Due to low OH absorption upon excitation at 3490 cm<sup>-1</sup>, we changed the solvent to nitrobenzene and increased the TDI and TCD concentration to about 0.25 mol/l.

The reaction rate measurements on CH-ol and PHI were performed with a 100 μm thin CaF<sub>2</sub> sample cell of 25 mm diameter. We used two identical sample cells filled with the same sample. One of the cells was irradiated by fs IR laser light (2 kHz repetition rate, 50 cm<sup>-1</sup> FWHM, and about 3 μJ energy), the other was not. For the irradiated cells we covered the complete chamber uniformly with IR light pulses by moving the sample line by line by a sample scanner. IR absorption spectra of the two samples

have been measured periodically with a 30-60 min interval with the Bruker spectrometer Equinox 55 for a duration of about 2 min. IR spectra at different temperatures were taken by changing the temperature with a chiller (see Supplementary Fig. 13). The average temperature within the IR excited sample volume was determined with a thermal imaging camera FLIR A600 under the same conditions as the reaction rate measurements, but with a non-moving sample (see Supplementary Fig. 12).

For the polymer square depicted in Fig. 5 the scanner was programmed to move the sample along the perimeter of a 4x4 mm or 3x3 mm square. Here, we used IR foci of 75 μm and 150 μm. Pictures of the polymer squares were taken with a camera (dnt DigiMicro Mobile) enable sizing of the polymer structures.

We used a home built IR light source to irradiate the sample for acceleration measurements<sup>36</sup>. This IR light source is a tunable optical parametric amplifier (OPA) generating high energy fs pulses of ~5 μJ in the range from 3.5 to 9 μm with pulse-length of about 350 fs, and a spectral width of ~ 50 cm<sup>-1</sup>. Femtosecond IR pump – IR probe experiments with pump frequencies below 2400 cm<sup>-1</sup> were performed with two independent home built IR light sources of this type<sup>36</sup>. Fs IR-pump IR-probe measurements on CH-ol and PHI with pump pulses at 3500 cm<sup>-1</sup> (see Supplementary Section 3.1.3) were conducted with home built IR light sources. IR pump beams were generated by cascaded tunable OPAs generating fs output pulses of ~3 μJ. In detail, a collinear BBO-OPA pumped at 400 nm generated near IR pulses at 1110 nm that were used to generate 2857 nm (3500 cm<sup>-1</sup>) pulses by two KTA amplification stages pumped with the fundamental at 800 nm. IR probe beams with an energy below 100 nJ were generated as reported elsewhere<sup>37</sup>. We used two probe beams to probe the same sample spot 1.5 ns before and fs to ps after IR excitation. The sample was moved with a Lissajous scanner to ensure a fresh sample volume at every pump beam.

In order to interpret the observed behavior, density functional theory (DFT) based calculations have been performed for the reaction between PHI and CH-ol. The solvent THF was included explicitly within the frame of the ONIOM model<sup>38</sup>. Details are provided in the Supplementary Section 2.

The data that support the findings of this study are available from the corresponding author upon reasonable request.

## References

- 1 Lin, J., Peng, Z., Liu, Y., Ruiz-Zepeda, F., Ye, R. Samuel, E. L. G., Yacaman, M. J., Yakobson, B. I. & Tour, J. M. Laser-induced porous graphene films from commercial polymers. *Nature Commun.* **5:5714**, 1-8 (2014).
- 2 Decker, C. & Elzaouk, B. Laser-induced crosslinking polymerization of acrylic photoresists. *J. Appl. Polym. Sci.* **65**, 833–844 (1997).
- 3 Malinauskas, M., Farsari, M., Piskarskas, A. & Juodkazis, S. Ultrafast laser nanostructuring of photopolymers: A decade of advances. *Phys. Rep.* **533**, 1-31 (2013).
- 4 Serbin, J., Egbert, A., Ostendorf, A., Chichkov, B. N., Houbertz, R., Domann, G., Schulz, J., Cronauer, C., Fröhlich, L. & Popall, M. Femtosecond laser-induced

- two-photon polymerization of inorganic-organic hybrid materials for applications in photonics. *Opt. Lett.* **28**, 301-303 (2003).
- 5 Li, L., Gattass, R. R., Gershgoren, E., Hwang, H. & Fourkas, J. T. Achieving  $\lambda/20$  resolution by one-color initiation and deactivation of polymerization. *Science* **324**, 910-913 (2009).
- 6 Gerasimov, T. G., Snavely, D. L. Vibrational Photopolymerization of Methyl Methacrylate and Quantitative Analysis of Polymerization Results. *Macromolecules* **35**, 5796-5800 (2002).
- 7 Gu, H. & Snavely, D. L. Vibrational Overtone Initiated Photopolymerization of Acrylonitrile. *J. Appl. Polym. Sci.* **90**, 565-571 (2003).
- 8 Crim, F. F. Selective Excitation Studies of Unimolecular Reaction Dynamics. *Ann. Rev. Phys. Chem.* **35**, 657-691 (1984).
- 9 Fleming, R. R. & Rizzo, T. R. Infrared spectrum of t-butyl hydroperoxide excited to the  $4\nu_{\text{OH}}$  vibrational overtone level. *J. Chem. Phys.*, **95**, 1461-1465 (1991).
- 10 Nesbitt, D. J. & Field, R. W. Vibrational Energy Flow in Highly Excited Molecules: Role of Intramolecular Vibrational Redistribution. *J. Chem. Phys.* **100**, 12735-12756 (1996).
- 11 Miller, Y., Chaban, G. M., Finlayson-Pitts, B. J. & Gerber, R. B. Photochemical Processes Induced by Vibrational Overtone Excitations: Dynamics Simulations for cis-HONO, trans-HONO, HNO<sub>3</sub>, and HNO<sub>3</sub>-H<sub>2</sub>O. *J. Phys. Chem. A* **110**, 5342-5354 (2006).
- 12 Koga, N. A review of the mutual dependence of Arrhenius parameters evaluated by the thermoanalytical study of solid-state reactions: the kinetic compensation effect. *Thermochim. Acta* **244**, 1-20 (1994).
- 13 Smith, I. W. M. The temperature-dependence of elementary reaction rates: beyond Arrhenius. *Chem. Soc. Rev.* **37**, 812-826 (2008).
- 14 Atkins, P.W. *Physical Chemistry* Vol.5, (Oxford University Press, 1994).
- 15 Dunning, G.T., Glowacki, D.R., Preston, T.J., Greaves, S.J., Greetham, G.M., Clark, I.P., Towrie, M., Harvey, J.N., Orr-Ewing, A.J. Vibrational relaxation and microsolvation of DF after F-atom reactions in polar solvents. *Science* **347**, 530-533 (2015).
- 16 González, L. & Kühn, O. in Handbook of Hydrogen Transfer, Hynes, J. T., Klinman, J. P., Limbach, H.-H., & Schowen, R. L. (eds.), Vol. 1, p. 79 (Wiley-VCH, Weinheim, 2006).
- 17 Shapiro, M. & Brumer, P. Quantum Control of Molecular Processes, 2nd edition (Wiley-VCH, Berlin, 2011).
- 18 Kühn, O. & Wöste, L. (eds.), Analysis and Control of Ultrafast Photoinduced Reactions, Series in Chemical Physics Vol. 87 (Springer Verlag, Berlin, 2007)
- 19 Ventalon, C., Fraser, J. M., Vos, M. H., Alexandrou, A, Martin, J.-L. & Joffre, M. Coherent vibrational climbing in carboxyhemoglobin. *Proc. Natl. Acad. Sci.* **101**, 13216-13220 (2004).
- 20 Strasfeld, D. B., Shim, S.-H. & Zanni, M. T. Controlling Vibrational Excitation with Shaped Mid-IR Pulses. *Phys. Rev. Lett.* **99**, 038102-038106 (2007).
- 21 Delor, M., Scattergood, P. A., Sazanovich, E. V., Parker, A. W., Greetham, G. M., Meijer, A. J. H. M., Towrie, M. & Weinstein, J. A. Toward control of electron transfer in donor-acceptor molecules by bond-specific infrared excitation. *Science* **346**, 1492-1495 (2014).
- 22 Lin, Z., Lawrence, C.M., Xiao, D., Kireev, V.V., Skourtis, S.S., Sessler, J.L., Beratan, D.N., Rubtsov, I.V. Modulating Unimolecular Charge Transfer by Exciting Bridge Vibrations. *J. Am. Chem. Soc.* **131**, 18060-18062 (2009).
- 23 Witte, T., Hornung, T., Windhorn, L., Proch, D., de Vivie-Riedle, R., Motzkus, M. & Kompa, K. L. Controlling molecular ground-state dissociation by optimal vibrational ladder climbing. *J. Chem. Phys.* **118**, 2021-2024 (2003).
- 24 Dian, B.C., Longarte, A., Zwier, T.S. Conformational Dynamics in a Dipeptide After Single-Mode Vibrational Excitation. *Science* **296**, 2369-2373 (2002).
- 25 Schanz, R., Božan, V., Hamm, P. A femtosecond study of the infrared-driven cis-trans isomerization of nitrous acid (HONO). *J. Chem. Phys.* **122**, 044509-10 (2005).
- 26 Heyne, K., Nibbering, E. T. J., Elsaesser, T., Petkovic, M. & Kühn, O. Cascaded energy redistribution upon O-H stretch excitation in an intramolecular hydrogen bonded system. *J. Phys. Chem. A* **108**, 6083-6086 (2004).
- 27 Rubtsov, I.V. Relaxation-Assisted Two-Dimensional Infrared (RA 2DIR) Method: Accessing Distances over 10 Å and Measuring Bond Connectivity Patterns. *Acc. Chem. Res.* **42**, 1385-1394 (2009).
- 28 Kasyanenko, V.M., Tesar, S.L., Rubtsov, G.I., Burin, A.L., Rubtsov, I.V. Structure Dependent Energy Transport: Relaxation-Assisted 2DIR Measurements and Theoretical Studies. *J. Phys. Chem. B* **115**, 11063-11073 (2011).
- 29 Kasyanenko, V.M., Keiffer, P., Rubtsov, I.V. Intramolecular vibrational coupling contribution to temperature dependence of vibrational mode frequencies. *J. Chem. Phys.* **136**, 144503 (2012).
- 30 Heyne, K., Huse, N., Dreyer, J., Nibbering, E.T.J., Elsaesser, T., Mukamel, S. Coherent low-frequency motions of hydrogen bonded acetic acid dimers in the liquid phase. *J. Chem. Phys.* **121**, 902 (2004).
- 31 Owrutsky, J.C., Raftery, D., and Hochstrasser, R. M. Vibrational Relaxation Dynamics in Solutions. *Annu. Rev. Phys. Chem.* **45**, 519-555 (1994).
- 32 Botan, V., Schanz, R. & Hamm, P. The infrared-driven cis-trans isomerization of HONO. II: Vibrational relaxation and slow isomerization channel. *J. Chem. Phys.* **124**, 234511-234519 (2006).
- 33 Windhorn, L., Yeston, J. S., Witte, T., Fuss, W., Motzkus, M., Proch, D., Kompa, K. L. & Moore, C. B. Getting ahead of IVR: A demonstration of mid-infrared molecular dissociation on sub-statistical timescale. *J. Chem. Phys.* **119**, 641-645 (2003).
- 34 Kössl, F., Lisaj, M., Kozich, V., Heyne, K. & Kühn, O. Monitoring the alcoholysis of isocyanates with infrared spectroscopy *Chem. Phys. Lett.* **621**, 411-45 (2015).

- 35 Heyne, K., Huse, N., Nibbering, E.T.J., Elsaesser, T. Ultrafast relaxation and anharmonic coupling of O-H stretching and bending excitations in cyclic acetic acid dimers. *Chem. Phys. Lett.* **382**, 19-25 (2003).
- 36 Kozich, V., Mogueilevski, A. & Heyne, K. High energy femtosecond OPA pumped by 1030 nm Yb:KGW laser. *Opt. Commun.* **285**, 285-289 (2012).
- 37 Kaindl, R.A., Wurm, M., Reimann, K., Hamm, P., Weiner, A.M., Woerner, M. Generation, shaping, and characterization of intense femtosecond pulses tunable from 3 to 20  $\mu\text{m}$ . *J. Opt. Soc. Am. B* **17**, 2086-2094 (2000).
- 38 Dapprich, S., Komáromi, I., Byun, K. S., Morokuma, K. & Frisch, M. J. A new ONIOM implementation in Gaussian98. Part I. The calculation of energies, gradients, vibrational frequencies and electric field derivatives. *J. Mol. Struct. (Theochem)* **462**, 1-21 (1999).

### Acknowledgements

The work was supported by the Deutsche Forschungsgemeinschaft (through grants No. Ku952/6 and He5206/3, CRC 1078 "Protonation Dynamics in Protein Function", Project B07, CRC 1114 "Scaling Cascades in Complex Systems", Project B05). We thank N.P. Ernsting for valuable discussion and the group of S. Reich for Raman microscopy experiments.

### Author contributions

T. S. performed the fs experiments on CH-ol and PHI, analyzed the data, and contributed to writing the paper. Y.Y. performed the fs experiments on CH-ol and PHI. V.K. performed acceleration measurements, photolithography measurements, analyzed the data, and contributed to writing the paper. F.K. provided the samples. A.A.A. performed the quantum chemical calculations, and analyzed their results, and contributed to writing the paper. K.H. and O.K. contributed to all measurements, calculations, and analysis, and wrote the paper. All authors commented on the manuscript.

### Additional information

Supplementary information is available in the online version of the paper. Correspondence and requests for materials should be addressed to K.H.

## Figure captions

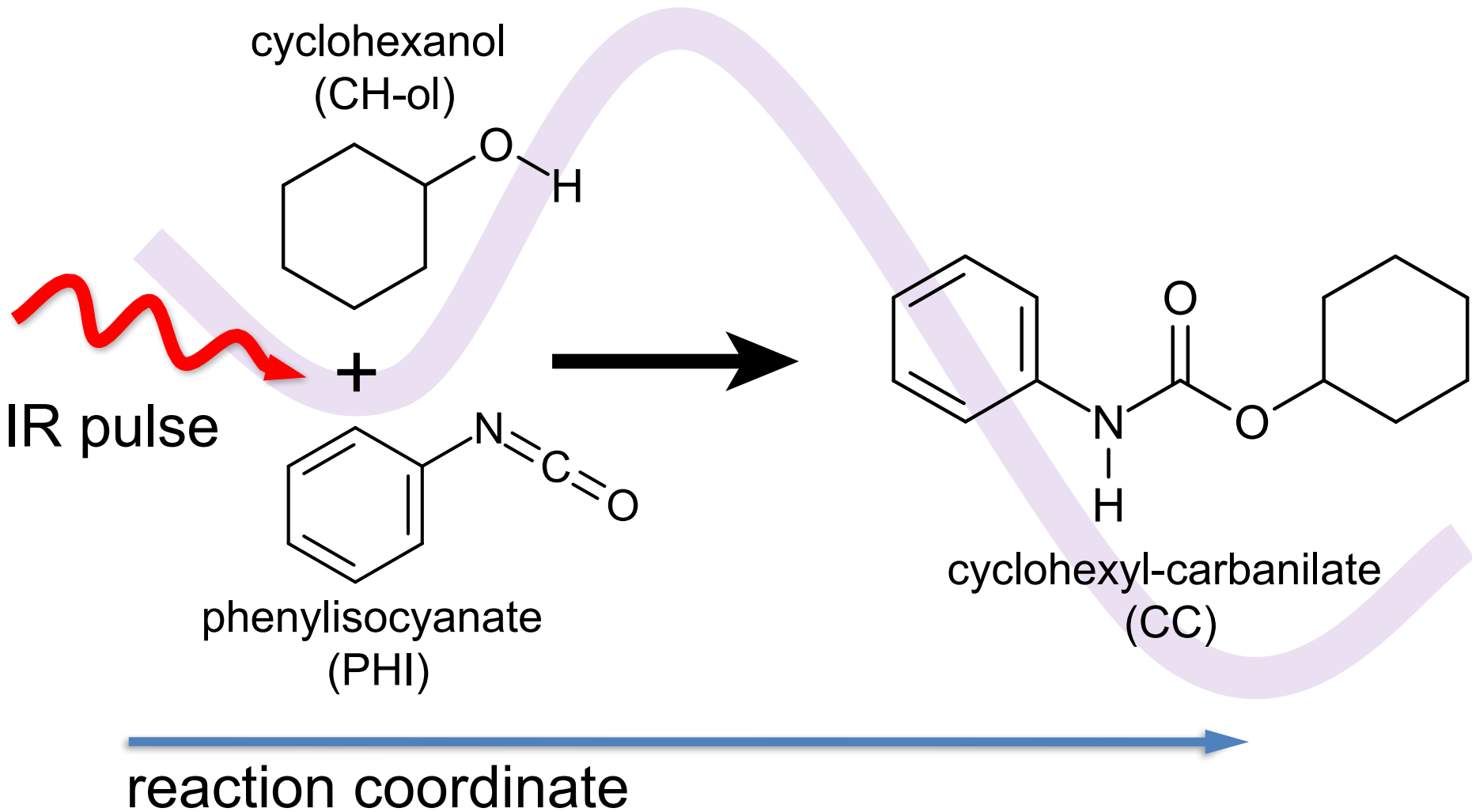
**Figure 1:** Schematic view of the IR-laser driven evolution along a reaction coordinate (RC) from reactants (PHI and CH-ol), via a transition state (TS) to the product (CC) for the present alcoholysis reaction.

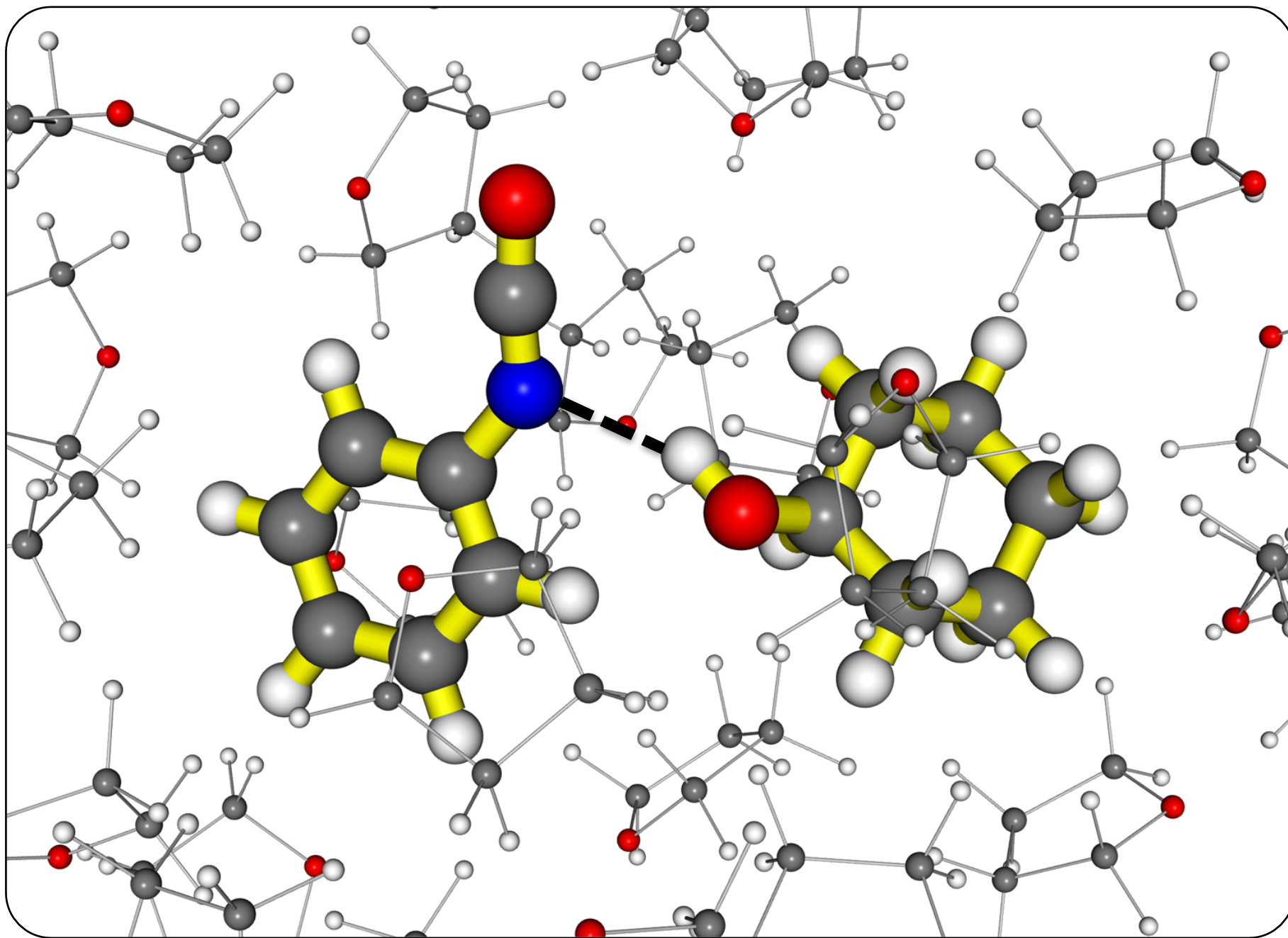
**Figure 2:** Energetics (in kcal/mol) and geometries for the reaction of PHI with CH-ol in THF for the reactant R1, R2, the transition state (TS), and the product CC. R2 and TS exhibit H-bonds between the NCO and OH group. Color code: blue (N), grey (C), red (O), white (H).

**Figure 3:** IR absorbance changes with time after mixing PHI and CH-ol without illumination (black lines) and with laser excitation at  $3500\text{ cm}^{-1}$  (red lines) for times at 0 min, and 300 min; PHI and CH-ol at 0.75 M concentration and 0.1 mm sample thickness. a) Absorption decrease of the OH-stretching vibration  $\nu(\text{OH})$  of CH-ol at  $3470\text{ cm}^{-1}$ , and absorption increase of the NH-stretching vibration  $\nu(\text{NH})$  of CC at  $3300\text{ cm}^{-1}$ . Illumination accelerates the consumption of CH-ol and formation of CC. b) Absorption increase of CC CO-stretching vibration  $\nu(\text{CO})$  at  $1730\text{ cm}^{-1}$ , and the NH-bending vibration  $\delta(\text{NH})$  at  $1505\text{ cm}^{-1}$ . Absorption decrease of the band at  $1512\text{ cm}^{-1}$ , due to a combination of NCO-stretching vibration  $\nu(\text{NCO})$  and CH-bending vibration  $\delta(\text{CH})$  of PHI. Illumination accelerates the consumption of PHI and formation of CC. Enlarged spectra with additional times are presented in Supplementary Fig. 14.

**Figure 4:** Absorbance difference spectra (dashed: zero line) averaged with respect to selected delay time intervals upon excitation of the CH-ol  $\nu(\text{OH})$  at  $3500\text{ cm}^{-1}$  of a 1:1 mixture of CH-ol and PHI in THF (a), (b). Difference between CH-ol/PHI and CH-ol/CC mixtures in THF upon excitation at  $3500\text{ cm}^{-1}$  (c). Decreased absorption (negative signals), increased absorption (positive signals). (a) Difference spectra in the region of the  $\nu(\text{NCO})$  &  $\delta(\text{CH})$  vibration at  $1512\text{ cm}^{-1}$  of PHI (scaled sample absorption, black line), and of the CC  $\delta(\text{NH})$  vibration at  $1505\text{ cm}^{-1}$ . Upon excitation of CH-ol the PHI vibration at  $1512\text{ cm}^{-1}$  decays, and the CC vibration at  $1505\text{ cm}^{-1}$  appears with about 10 ps; (b) difference spectra in the region of the  $\nu(\text{NCO})$  vibration at  $2270\text{ cm}^{-1}$  of PHI (scaled sample absorption, black line). Upon excitation of CH-ol the  $\nu(\text{NCO})$  vibration of PHI decays with about 10 ps; (c) double difference spectra in the region of the  $\nu(\text{CO})$  vibration at  $1730\text{ cm}^{-1}$  of CC (scaled sample absorption of a reacted sample, black line). Upon excitation of CH-ol the  $\nu(\text{CO})$  vibration is formed with a time constant of 10 ps, displaying CC formation. Bleaching of PHI bands and formation of CC vibrations upon CH-ol excitation with 10 ps show IR pulse induced alcoholysis reaction. Transients are presented in Supplementary Figs. 21 and 22. Errors of the averaged delay time intervals are indicated.

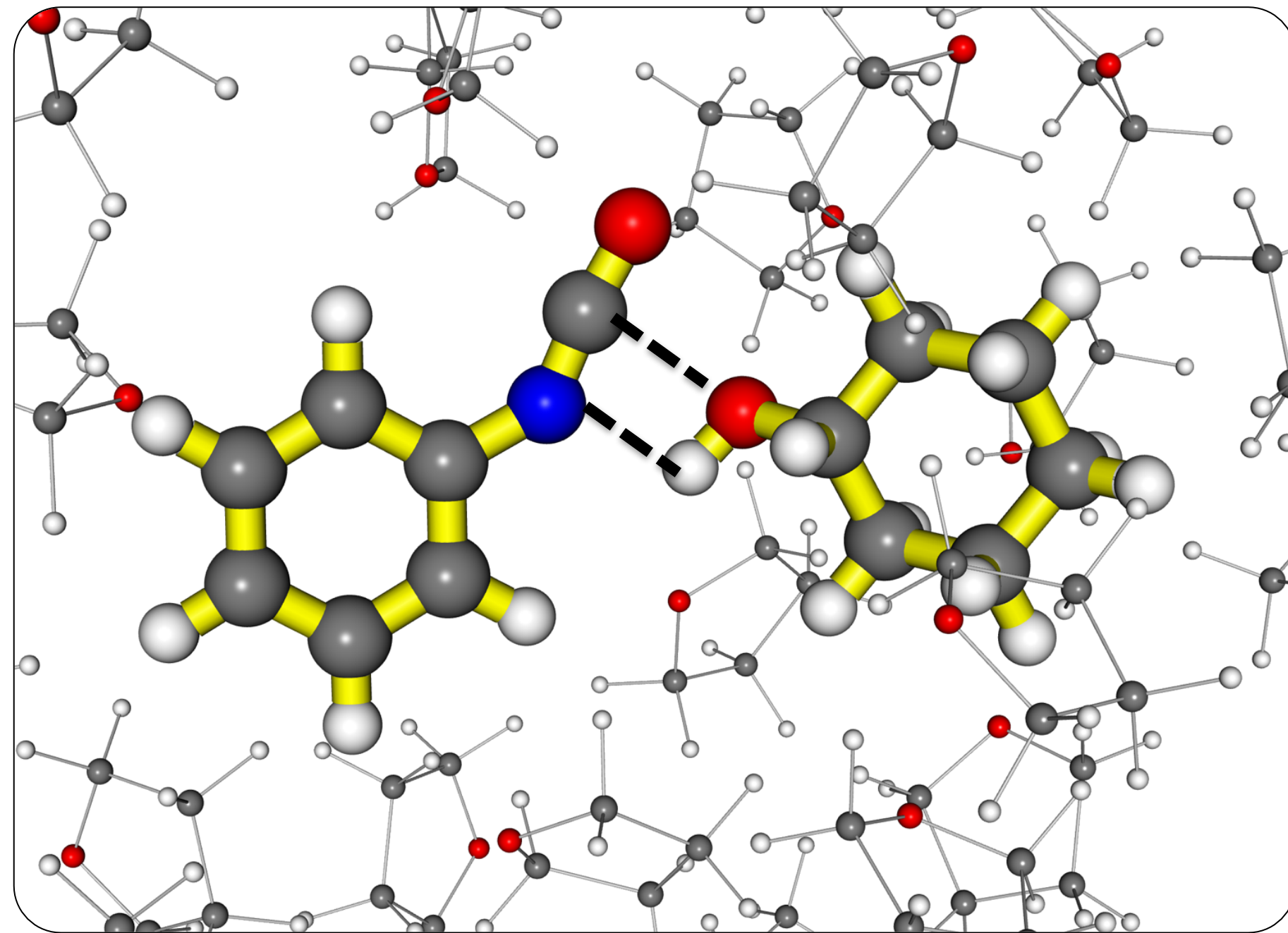
**Figure 5:** Polyurethane square generated upon IR excitation of a TDI and TCD solution at  $2270\text{ cm}^{-1}$  due to IR pulse induced reaction acceleration. Writing a  $4 \times 4\text{ mm}$  square with a focal diameter of  $150\text{ }\mu\text{m}$ ; inset: Writing a  $3 \times 3\text{ mm}$  square with a focal diameter of  $75\text{ }\mu\text{m}$ . Yellow bars indicate the different polymer line width of  $\approx 160\text{ }\mu\text{m}$  (upper bars) and  $\approx 80\text{ }\mu\text{m}$  (lower bars, see also Supplementary Fig. 23). The line width of the polymer follows the focal diameter of the IR light.





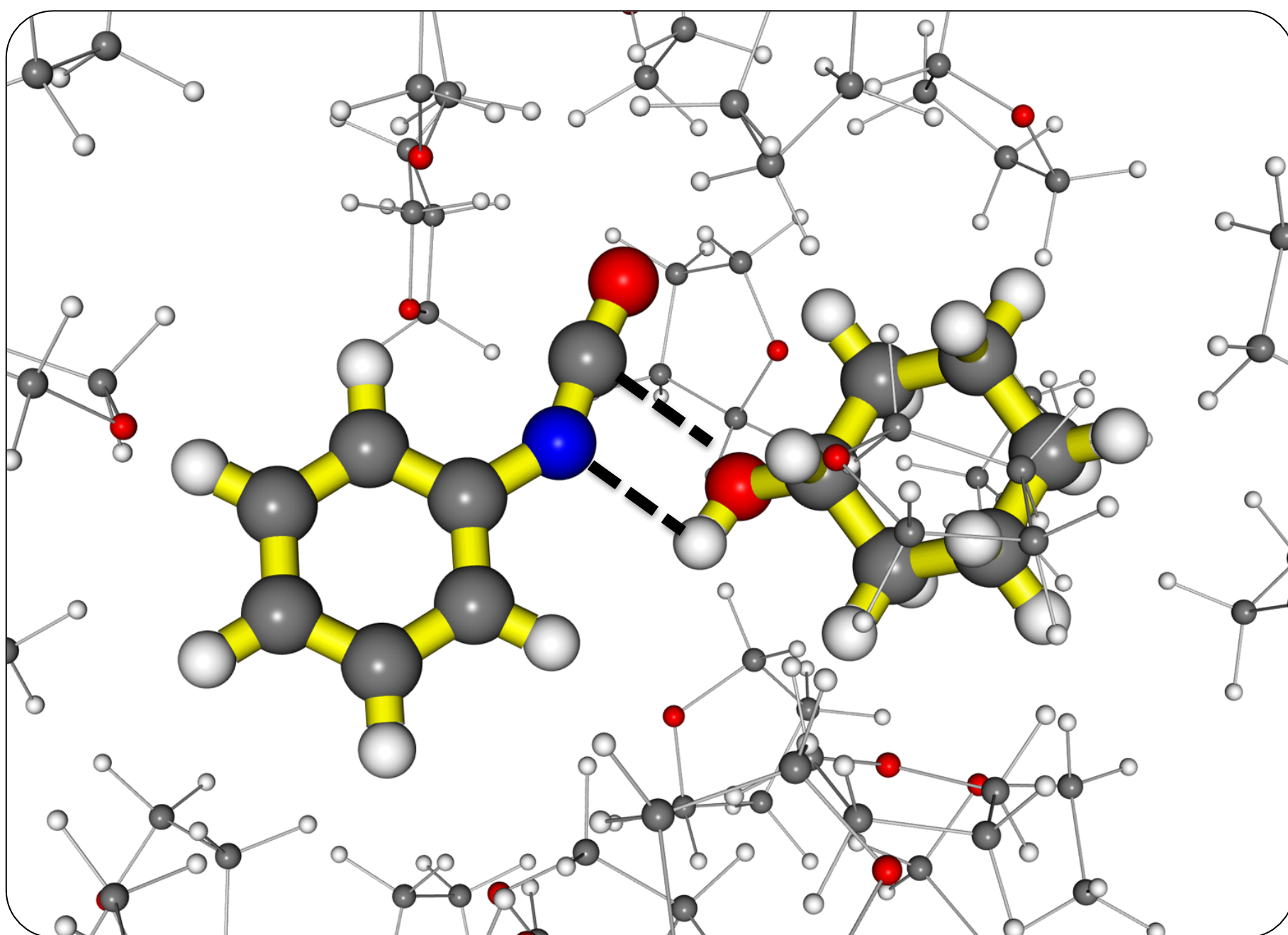
**Reactant1 (R1)**

$$\Delta G(\text{R1} \rightarrow \text{TS}) = 13.4 \text{ kcal/mol}$$



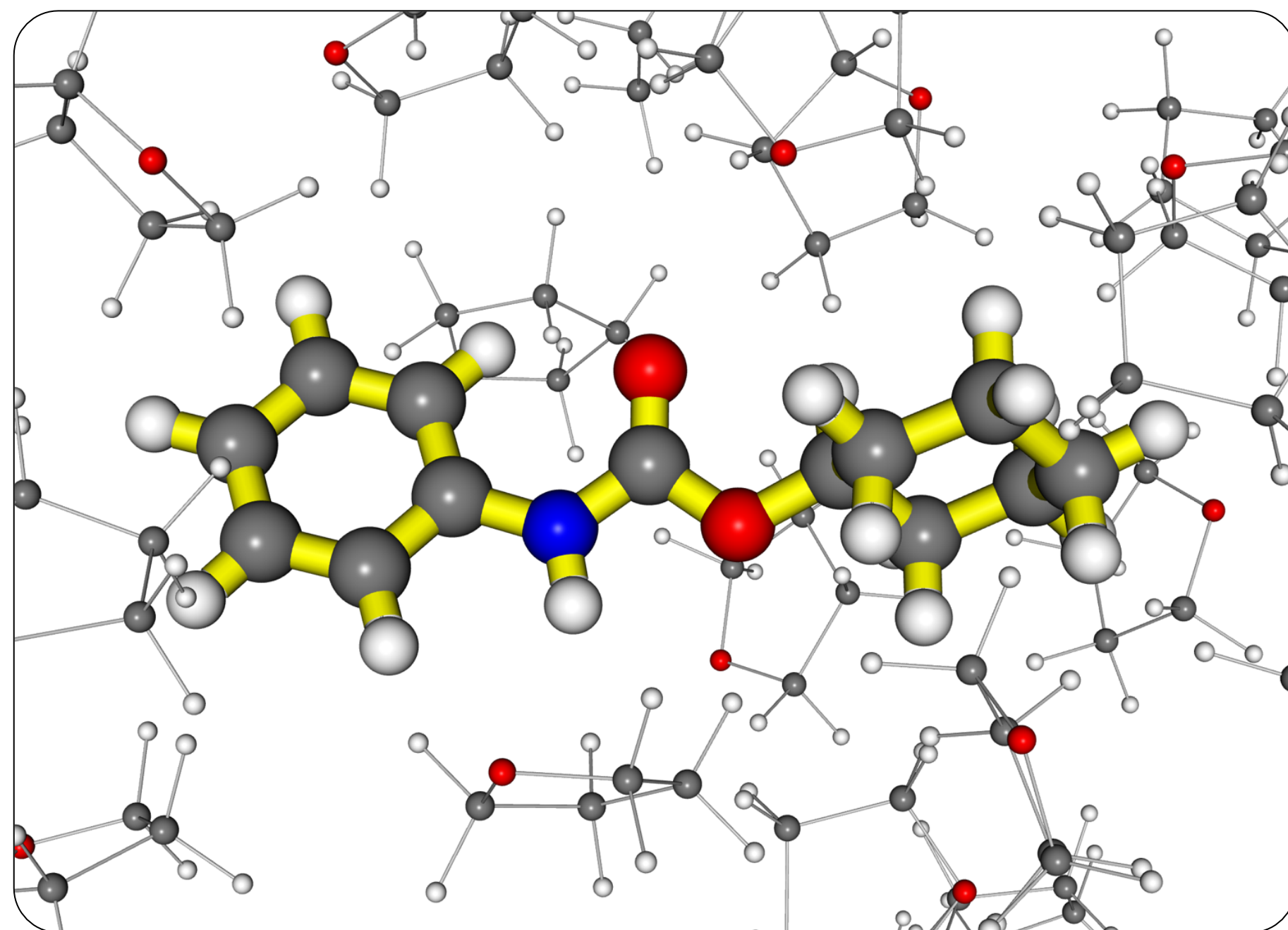
**Reactant2 (R2)**

$$\Delta G(\text{R2} \rightarrow \text{TS}) = 6.8 \text{ kcal/mol}$$



**Transition State (TS)**

$$\Delta G(\text{TS} \rightarrow \text{P}) = -30.7 \text{ kcal/mol}$$



**Product (P)**

